

Theory of nonreciprocal spin-wave excitations in spin Hall oscillators with Dzyaloshinskii-Moriya interaction

R. Zivieri,¹ A. Giordano,¹ R. Verba,² B. Azzerboni,³ M. Carpentieri,⁴ A. N. Slavin,⁵ and G. Finocchio^{1,*}

¹*Department of Mathematical and Computer Sciences, Physical Sciences and Earth Sciences, University of Messina, Messina, Italy*

²*Institute of Magnetism, Kyiv 03680, Ukraine*

³*Department of Engineering, University of Messina, Messina, Italy*

⁴*Department of Electrical and Information Engineering, Politecnico di Bari, I-70125 Bari, Italy*

⁵*Department of Physics, Oakland University, Rochester, Michigan 48309, USA*



(Received 27 February 2018; published 18 April 2018)

A two-dimensional analytical model for the description of the excitation of nonreciprocal spin waves by spin current in spin Hall oscillators in the presence of the interfacial Dzyaloshinskii-Moriya interaction (*i*-DMI) is developed. The theory allows one to calculate the threshold current for the excitation of spin waves, as well as the frequencies and spatial profiles of the excited spin-wave modes. It is found that the frequency of the excited spin waves exhibits a quadratic redshift with the *i*-DMI strength. At the same time, in the range of small and moderate values of the *i*-DMI constant, the averaged wave number of the excited spin waves is almost independent of the *i*-DMI, which results in a rather weak dependence on the *i*-DMI of the threshold current of the spin-wave excitation. The obtained analytical results are confirmed by the results of micromagnetic simulations.

DOI: [10.1103/PhysRevB.97.134416](https://doi.org/10.1103/PhysRevB.97.134416)

I. INTRODUCTION

In recent years, the excitation of microwave magnetization oscillations driven by a spin-polarized electric current or pure spin current has attracted much attention, both among theoreticians and experimentalists. Magnetization dynamics in spin torque oscillators (STOs) and spin Hall oscillators (SHOs) can exhibit various types of behavior, including highly nonlinear and nonstationary dynamics [1–3], making these oscillators an interesting test system for the investigation of nonlinear phenomena in ferromagnets. At the same time, STOs and SHOs demonstrate properties that make them suitable for a wide range of applications, such as generators of microwave signals [4–10], neuromorphic computing [11], microwave-assisted magnetic recording [12], etc.

The STOs and SHOs, in which spin-polarized electric current (or pure spin current) is injected locally in an unbounded ferromagnetic layer, are an important class of oscillators [13–15], because *propagating* spin waves can be excited in these oscillators in the case of out-of-plane magnetization [16–24]. The excitation of *propagating* spin waves makes these oscillators promising for signal processing applications in all spin-wave logic [25] and magnonics [26], and for the development of large arrays of phase-locked auto-oscillators efficiently coupled by the propagating spin waves [27–29].

In the case when the SHO free layer is influenced by the interfacial Dzyaloshinskii-Moriya interaction [30,31] (*i*-DMI), which is an antisymmetric exchange interaction, appearing at the interface between a ferromagnet and a heavy metal with large spin-orbit coupling [32], the SHO could acquire

an additional functionality. The *i*-DMI is known to introduce frequency nonreciprocity into the spectrum of propagating spin waves [32–36], leading to several potential physical and technological implications, such as the creation of unidirectional spin-wave emitters, the separation of signal and idler waves in frequency and wave-number domains in spin-wave devices, which use parametric and nonlinear spin-wave processes, etc. [37–40]. In recent theoretical works [41,42], it has been shown that the *i*-DMI in STO and SHO results in the excitation of two-dimensional nonreciprocal spin waves, and, at a sufficient strength of the *i*-DMI, in the generation of spiral spin-wave modes.

The main purpose of this paper is the development of an analytical model, which describes the excitation of *two-dimensional* nonreciprocal spin waves in a nanocontact SHO (the quasi-one-dimensional case of a nanowire-based SHO has been already considered theoretically in Ref. [41]). Our approach is based on an approximate solution of the linearized Landau-Lifshitz-Gilbert-Slonczewski (LLGS) equation and, in fact, is a generalization of the Slonczewski's theory [16] to the case of the presence of the *i*-DMI. The developed theory allows one to calculate profiles of the excited spin waves, which are approximately described by a combination of Laguerre's polynomials and Tricomi's hypergeometric functions, as well as to calculate the excitation threshold and frequency of excited spin waves, both of which become lower with increased *i*-DMI strength.

The paper is organized as follows. Section II describes the model system used in this study. In Sec. III, a step-by-step derivation of the analytical formalism is presented. Analytically calculated results are compared with micromagnetic modeling in Sec. IV. Finally, conclusions are given in Sec. V.

*gfinocchio@unime.it

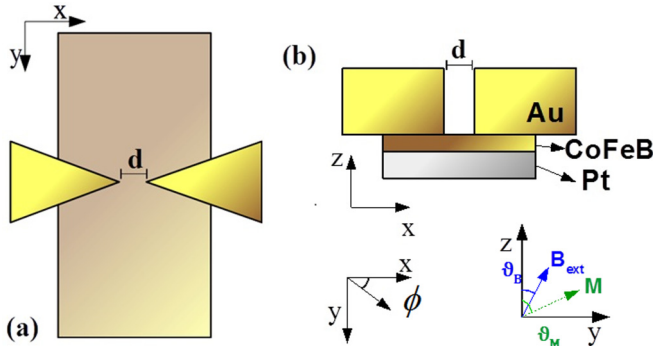


FIG. 1. Sketch of the device under investigation. (a) x - y in-plane view and (b) x - z cross section. The indication of azimuthal angle ϕ related to the wave vector, the direction of the applied field \mathbf{B}_{ext} , the angle θ_B , and the angle θ_M of the equilibrium magnetization \mathbf{M} vector are also shown.

II. DEVICE UNDER STUDY AND MICROMAGNETIC SIMULATIONS

The device under investigation is shown in Fig. 1. It is a typical SHO, consisting of a ferromagnetic/heavy-metal bilayer. The current is injected locally in the bilayer by using a gold concentrator of a double-triangular shape with a distance d between the tips. The system is biased by an external magnetic field \mathbf{B}_{ext} , applied in the y - z plane and making the angle θ_B with the film normal (axis z) [Fig. 1(b)]. A bias magnetic field is required in order to tilt the film static magnetization from the in-plane direction, and, if the angle θ_M between the static magnetization and film normal is sufficiently small, the SHO supports the excitation of propagating spin waves. Otherwise, either a nonlinear self-localized bullet mode is excited due to the negative nonlinear frequency shift, or a transient regime of mode coexistence is realized [19,43].

In our micromagnetic simulations we used the parameters of a Pt(5 nm)/CoFeB(1 nm) bilayer, having a rectangular in-plane cross section of $1500 \text{ nm} \times 3000 \text{ nm}$. The gold concentrator was assumed to be 150 nm thick, with the distance between the tips of $d = 100 \text{ nm}$. Details on the calculation of the electric current and the spin current profiles can be found in Ref. [41]. For the material parameters of the ferromagnetic layer we assumed a gyromagnetic ratio $\gamma = 2\pi \times 28 \text{ GHz/T}$, saturation magnetization $M_S = 1000 \times 10^3 \text{ A/m}$, exchange stiffness $A = 2.0 \times 10^{-11} \text{ J/m}$, constant of perpendicular surface anisotropy $K_s = 5.5 \times 10^{-4} \text{ J/m}^2$ (resulting in an effective volume anisotropy of $K_u = 5.5 \times 10^5 \text{ J/m}^3$), a Gilbert damping parameter $\alpha_G = 0.03$, and a spin Hall angle $\alpha_H = 0.1$. The i -DMI parameter D was varied in a range [44] in order to systematically study its effect on the nonreciprocal propagation of spin waves. Experimentally, an i -DMI parameter variation can be realized by the variation of the ferromagnetic film thickness or by use of a different material, covering the ferromagnetic film from another side. The external bias magnetic field was applied at an angle $\theta_B = 15^\circ$. For these parameters, the CoFeB layer had an easy-plane total (material plus shape) anisotropy. It is known that a partial compensation of the demagnetization field by perpendicular anisotropy allows one to reduce the critical

current density necessary to excite propagating spin-wave modes in a tilted external field [38]. All the micromagnetic simulations in this study have been performed using a state-of-the-art micromagnetic solver [45].

III. ANALYTICAL MODEL

In this section, we present a two-dimensional analytical model developed to study the nonreciprocal propagation of spin waves in the presence of an i -DMI interaction. In Sec. III A, we derive the linearized dynamical equation of motion for the magnetization, describing the spatial and temporal dependence of the spin-wave amplitude. Section III B is devoted to the general solution of the linearized equation of motion to obtain the analytical expression for the spatial profiles of the two-dimensional spin-wave mode, and to determine its angular-dependent wave number and group velocity. Section III C describes the calculation of the angular-dependent spin-wave wave vector, highlighting the influence of the i -DMI. In Sec. III D, the computation of the threshold current density is described, and the explicit quadratic dependence of the generation frequency on the i -DMI parameter is found. Finally, in Sec. III E, the main equations of our theoretical model are analyzed.

A. Initial equations

The dynamics of magnetization $\mathbf{M}(\mathbf{r}, t)$ of a ferromagnetic layer under the influence of spin current is described by the LLGS equation,

$$\frac{d\mathbf{M}}{dt} = \gamma \mathbf{B}_{\text{eff}} \times \mathbf{M} + \frac{\alpha_G}{M_S} \mathbf{M} \times \frac{d\mathbf{M}}{dt} - \frac{g\mu_B\alpha_H}{2eM_S^2 t_{\text{FM}}} \mathbf{M} \times \mathbf{M} \times (\mathbf{e}_z \times \mathbf{J}), \quad (1)$$

where g is the Landè factor, μ_B is the Bohr magneton, e is the electron charge, t_{FM} is the thickness of the ferromagnetic layer, α_H is the spin Hall angle, and \mathbf{J} is the electric current density flowing in the Pt layer. The effective field \mathbf{B}_{eff} includes the contributions of external field \mathbf{B}_{ext} , demagnetization, exchange, and i -DMI contributions ($\mathbf{B}_{i\text{-DMI}} = 2D/M_S^2[(\nabla \cdot \mathbf{M})\mathbf{e}_z - \nabla M_z]$, where D is the i -DMI constant).

Equation (1) is used in micromagnetic simulations, but it is too complex for the analytic analysis. From Eq. (1) one can derive a dispersion relation of linear spin waves propagating in the ferromagnetic film (for this purpose one needs to neglect the last two nonconservative terms and to represent the full magnetization of the film as a sum of its static magnetization and a small dynamic deviation) [46],

$$\omega_k = \sqrt{(\omega_H + \omega_M \lambda^2 k^2)(\omega_H + \omega_M \lambda^2 k^2 + \omega_M(1 - N_{\text{an}})\sin^2 \theta_M)} + \omega_M \tilde{D} k_x, \quad (2)$$

where \mathbf{k} is the wave vector of a spin wave, $\omega_H = \gamma B_{\text{eff}}$, B_{eff} is the modulus of the effective static magnetic field, $\omega_M = \gamma \mu_0 M_S$, $N_{\text{an}} = 2K_u/(\mu_0 M_S^2)$ where K_u is the anisotropy constant, $\lambda = \sqrt{2A/(\mu_0 M_S^2)}$ is the material exchange length, and $\tilde{D} = 2D \sin \theta_M/(\mu_0 M_S^2)$ is the normalized i -DMI constant. One can see that the nonreciprocity, induced by the i -DMI, depends on the magnetization angle, and disappears in the case

of perpendicular static magnetization ($\theta_M = 0$). Therefore, it is desirable to choose a large magnetization angle, which, however, should be smaller than the critical value, corresponding to the change of sign of the nonlinear frequency shift from positive to negative, so that the propagating spin waves could be excited [19,23]. Since we consider an ultrathin ferromagnetic film, the in-plane dynamic dipolar contribution is neglected in Eq. (2). In the range $\omega_M \lambda^2 k^2 \ll \omega_0$, the dispersion relation can be approximated as

$$\omega_k \approx \omega_0 + \omega_M \tilde{\lambda}^2 k^2 + \omega_M \tilde{D} k_x, \quad (3)$$

where $\omega_0 = \sqrt{\omega_H[\omega_H + \omega_M(1 - N_{\text{an}})\sin^2\theta_M]}$ is the ferromagnetic resonance frequency and $\tilde{\lambda}^2 = \lambda^2[2\omega_H + \omega_M(1 - N_{\text{an}})\sin^2\theta_M]/2\omega_0$.

Making a formal substitution $k_x \rightarrow -i(d/dx)$, $k_y \rightarrow -i(d/dy)$ in the simplified dispersion equation, it is possible to obtain the following dynamical equation describing the spatial and temporal evolution of the spin-wave complex amplitude $a = a(x, y)$,

$$\begin{aligned} \frac{\partial a}{\partial t} = & -i\omega a = -i\left(\omega_0 - \omega_M \tilde{\lambda}^2 \nabla^2 - i\omega_M \tilde{D} \frac{\partial}{\partial x}\right)a \\ & - \alpha_G \omega a + \sigma J(\mathbf{r})a, \end{aligned} \quad (4)$$

which differs from the one used by Slonczewski [16] by the presence of the i -DMI term. The spin-wave damping is accounted for by the term $\alpha_G \omega$, while the influence of the spin current could be easily calculated from Eq. (1) within the framework of the perturbation theory [47], and is given by the term $\sigma J(\mathbf{r})a$ with the coefficient $\sigma = g\mu_B \alpha_H \sin\theta_M / (2eM_S t_{\text{FM}})$, describing the spin Hall efficiency and $\mathbf{r} = (x, y)$.

We have not included the Oersted field in the model (which results in a spatial dependence of ω_0), because it does not introduce any qualitative change [41]. Thus, the only spatially dependent parameter in Eq. (4) is the distribution of the current density. We approximate it in a cylindrical system (see Sec. III B) with the function $J(r) = J$ if $r < R_{\text{eff}}$ and $J(r) = 0$ otherwise with r the radial coordinate, i.e., we assume that current is flowing only within a circle of the radius R_{eff} . For spin Hall oscillators with concentrators such as the one shown in Fig. 1 it is an approximation, and the value of the effective radius R_{eff} , which is of the order of the half distance between the concentrator tips, should be determined by comparison with simulations (see Sec. IV). Simultaneously, such a case can be exactly realized in an STO [42].

B. General solution of the eigenvalue problem

Equation (4) can be considered as an eigenvalue problem, whose solution gives the values of the spin-wave excitation frequency ω and the critical current J . In the considered geometry it is convenient to express Eq. (4) in cylindrical coordinates (ρ, ϕ) ,

$$\begin{aligned} \left(\frac{\partial^2}{\partial \rho^2} + \frac{1}{\rho} \frac{\partial}{\partial \rho} + \frac{1}{\rho^2} \frac{\partial^2}{\partial \phi^2}\right)a + i\tilde{A} \left(\cos\phi \frac{\partial}{\partial \rho} - \frac{\sin\phi}{\rho} \frac{\partial}{\partial \phi}\right)a \\ + (W + iG)a = 0. \end{aligned} \quad (5)$$

Here, we introduce a dimensionless coordinate $\rho = r/R_{\text{eff}}$, and the following dimensionless parameters: $\tilde{A} =$

$\tilde{D} R_{\text{eff}}/\tilde{\lambda}^2$, describing the strength of the i -DMI, $W = (\omega - \omega_0)R_{\text{eff}}^2/(\omega_M \tilde{\lambda}^2)$, proportional to the generation frequency offset from the ferromagnetic resonance (FMR) frequency, and the normalized total damping G , which is equal to $G_1 = (\alpha_G \omega - \sigma J)R_{\text{eff}}^2/(\omega_M \tilde{\lambda}^2)$ within the active region ($\rho < 1$) and to $G_2 = (\alpha_G \omega)R_{\text{eff}}^2/(\omega_M \tilde{\lambda}^2)$ outside the active region.

Equation (5) does not allow an exact analytical solution, because the dependencies on the radial and azimuthal coordinates cannot be separated due to the presence of the i -DMI term. At the same time, in the absence of the i -DMI, this separation can be done rigorously, and the solution, corresponding to the lowest excitation threshold, has a simple form $a = a(\rho)$, i.e., it is radially symmetric, and does not depend on the azimuthal angle ϕ . Hence, we can assume that, at least in the range of a relatively weak i -DMI, the radially symmetric solution is only weakly modified, and the dependence on ϕ is also weak. This approximation allows us to consider the azimuthal coordinate not as an independent variable, but as a parameter which affects the radially symmetric solution $a = a_\phi(\rho)$, i.e., to neglect the derivative $\partial/\partial\phi$ in Eq. (4). As will be shown below, this approximation leads to correct dependencies of the generation frequency and threshold in the i -DMI range of interest.

Owing to the mentioned approximation, Eq. (5) is simplified to

$$\left(\frac{\partial^2}{\partial \rho^2} + \frac{1}{\rho} \frac{\partial}{\partial \rho} + i\tilde{A} \cos\phi \frac{\partial}{\partial \rho}\right)a + (W + iG)a = 0. \quad (6)$$

Equation (6) is a generalized confluent Riemann hypergeometric equation. Its general solution is a linear combination of a Laguerre's polynomial L (often known as a particular form of a Kummer's hypergeometric function) and a confluent hypergeometric function U (often known as a Tricomi's hypergeometric function) times an exponential function, namely,

$$\begin{aligned} a_\phi(\rho) = e^{-i(\alpha+\beta)\rho/2} \left[C_1 L\left(-\frac{1}{2} - \frac{\alpha}{2\beta}, i\beta\rho\right) \right. \\ \left. + C_2 U\left(\frac{1}{2} + \frac{\alpha}{2\beta}, 1, i\beta\rho\right) \right], \end{aligned} \quad (7)$$

where the parameters α and β are defined as $\alpha = \tilde{A} \cos\phi$ and $\beta_{1,2} = \sqrt{4(W + iG_{1,2}) + \tilde{A}^2 \cos^2\phi}$. The coefficients C_1, C_2 should be determined from the boundary conditions and proper asymptotes. Since the function U is divergent at $\rho \rightarrow 0$, the solution in the active region ($\rho < 1$) is given by the Laguerre's polynomial solely,

$$a_{\phi,1}(\rho) = e^{-i(\alpha+\beta_1)\rho/2} L\left(-\frac{1}{2} - \frac{\alpha}{2\beta_1}, i\beta_1\rho\right). \quad (8)$$

The solution outside the active region should have the asymptotic form of a decaying propagating wave, i.e., $a_{\phi,2}(\rho) \sim \rho^{-1/2} e^{i\kappa\rho} e^{-c_g G_2 \rho}$ with $c_g > 0$. This property is satisfied by the following combination,

$$\begin{aligned} a_{\phi,2}(\rho) = C e^{-i(\alpha+\beta_2)\rho/2} \left[L\left(-\frac{1}{2} - \frac{\alpha}{2\beta_2}, i\beta_2\rho\right) \right. \\ \left. - \frac{i^{1+\alpha/\beta_2}}{\Gamma[1/2 - \alpha/(2\beta_2)]} U\left(\frac{1}{2} + \frac{\alpha}{2\beta_2}, 1, i\beta_2\rho\right) \right], \end{aligned} \quad (9)$$

where $\Gamma[x]$ is the gamma function. The coefficient C is determined by the continuity of the solution at the boundary of the active region $a_{\phi,1}(1) = a_{\phi,2}(1)$. In the case of zero i -DMI, $\alpha = 0$, the above solutions are simplified to $a_1(\rho) = J_0(\beta_1\rho/2)$ and $a_2(\rho) = CH_0^{(1)}(\beta_2\rho/2)/2$, respectively, where J_0 and $H_0^{(1)}$ are the Bessel and Hankel functions of the zero order, which is in full accordance with Refs. [16,48].

C. Angular dependence of spin-wave wave number

Using asymptotic expansions of Laguerre polynomial and hypergeometric function, one can show that at $\rho \gg 1$ the solution expressed in Eq. (9) behaves as $a_{\phi,2}(\rho) \sim \rho^{-1/2-\alpha/2\beta_2} \exp[i(\beta_2 - \alpha)\rho/2]$, i.e., has a form of a wave, propagating from a point source, and having an angular-dependent wave number, which is determined by the term $\exp[ik_\phi r]$. The wave number is equal to $k_\phi = \text{Re}[\beta_2 - \alpha]/(2R_{\text{eff}})$, or, in the initial parameters, can be expressed as

$$k_\phi = \frac{1}{2\tilde{\lambda}^2} \left[-\tilde{D} \cos \phi + \sqrt{4 \frac{\omega - \omega_0}{\omega_M} \tilde{\lambda}^2 + \tilde{D}^2 \cos^2 \phi} \right]. \quad (10)$$

This expression can be also directly obtained from the spin-wave spectrum Eq. (3), which confirms the correct asymptotic behavior of the solution given by Eqs. (8) and (9). The exponential decay of the spin waves, caused by damping, is described by the term $\exp[-\alpha_G r/v_{\text{gr}}]$, with

$$v_{\text{gr}} = \omega_M(2\tilde{\lambda}^2 k + \tilde{D} \cos \phi) \quad (11)$$

being the spin-wave group velocity (to derive this expression we used the assumption of small damping, $\alpha_G \ll 1$).

The dependence of the spin-wave wave number on the azimuthal angle is nonreciprocal, in the sense that $k_\phi \neq k_{\pi-\phi}$, which is a consequence of the i -DMI. The averaged value of the wave number is equal to

$$\langle k \rangle = \frac{\sqrt{4(\omega - \omega_0)\tilde{\lambda}^2/\omega_M + \tilde{D}^2}}{\pi\tilde{\lambda}^2} E \left[\frac{\tilde{D}^2\omega_M}{4(\omega - \omega_0)\tilde{\lambda}^2 + \tilde{D}^2\omega_M} \right], \quad (12)$$

where $E[m]$ is the complete elliptic integral of the second kind. For small i -DMI it is simplified to $\langle k \rangle = \sqrt{4(\omega - \omega_0)\tilde{\lambda}^2/\omega_M + \tilde{D}^2}/(2\tilde{\lambda}^2)$. In the section below, we will find the excitation frequency ω , and will show that the averaged value of the spin-wave wave number is almost independent of \tilde{D} in the range of a relatively weak i -DMI.

D. Determination of the threshold current and generation frequency

The generation frequency and threshold current density can be determined by the application of the boundary conditions to the general solution Eqs. (8) and (9). The boundary conditions require continuity of the function $a_\phi(\rho)$ and its derivative at the boundary of the active region ($\rho = 1$). The first condition is satisfied automatically by the selection of the coefficient C in Eq. (9). However, since we use approximate solutions, the condition on the derivatives $da_{\phi,1}/d\rho|_{\rho=1} = da_{\phi,2}/d\rho|_{\rho=1}$ cannot be satisfied exactly for all the azimuthal angles ϕ simultaneously by any values of the generation frequency and the bias current density. Therefore, instead of the condition

of the exact matching of derivatives, we use the condition of the minimization of a total mismatch of the derivatives. This approach is analogous to the collocation and least squares method used to approximate numerical solutions of differential and integral equations [49–51].

For this purpose, we construct the functional of the quadratic deviation of the derivatives at the boundary of the active region,

$$\Phi[W, G_1] = \int_0^{2\pi} |\mathcal{F}(\phi)|^2 d\phi, \quad (13)$$

where

$$\mathcal{F}(\phi) = \left(\frac{da_{\phi,1}}{d\rho} - \frac{da_{\phi,2}}{d\rho} \right) \Big|_{\rho=1}. \quad (14)$$

The normalized generation frequency W and the threshold G_1 are then given by the minimum of $\Phi[W, G_1]$.

Let us find an analytical approximation for the generation frequency and threshold. Taking into account the structure of the functions $a_{\phi,i}(\rho)$, we can consider the function \mathcal{F} as the function of three variables, $\alpha = \tilde{A} \cos \phi$, β_1 , and β_2 . The value of α is proportional to the i -DMI strength, which is considered relatively small in the model. Thus, we can expand the function \mathcal{F} in a series leaving only a linear term in α , namely, $\mathcal{F} = \mathcal{F}_0 + C_f \tilde{A} \cos \phi$, where $\mathcal{F}_0 = \mathcal{F}(\tilde{A} = 0)$. After the integration, one gets $\Phi = \int_0^{2\pi} |\mathcal{F}_0|^2 d\phi + |C_f|^2 \tilde{A}^2/2$. Consequently, the condition of the function minimum $\partial\Phi/\partial W = \partial\Phi/\partial G_1 = 0$ does not depend on C_f . This means that we can set $\alpha = 0$ in the definition of the function \mathcal{F} , at least for a small i -DMI. This property is, in fact, more general—the generation frequency and threshold should be the same for i -DMI of the same strength but opposite values, because the change $D \rightarrow -D$ corresponds to the simple inversion of the x axis. Thus, odd functions of D can be safely disregarded.

Setting $\alpha = 0$, the function in Eq. (13) is simplified to

$$\mathcal{F} = \frac{\beta_1}{2} J_0\left(\frac{\beta_1}{2}\right) H_1^{(1)}\left(\frac{\beta_2}{2}\right) - \frac{\beta_1}{2} J_1\left(\frac{\beta_1}{2}\right) H_0^{(1)}\left(\frac{\beta_2}{2}\right). \quad (15)$$

Following Ref. [16], we first consider the case of zero Gilbert damping. Then, the function of Eq. (15) has exact zero at the values $W + \tilde{A}^2 \cos^2 \phi/4 \approx 1.43$ and $G_1 = -\sigma J R_{\text{eff}}^2/(\omega_M \tilde{\lambda}^2) \approx -1.86$. One can see that the value of the normalized threshold current G_1 does not depend on the angle ϕ , thus it is the solution of the problem of minimization of the functional Φ . Since we disregard Gilbert damping at this moment, the found value of the current density J corresponds to the compensation of the radiation losses, and, as we see, this threshold value does not depend on the i -DMI. This feature will be explained below.

The last step is finding the generation frequency W . As it was pointed out, $\mathcal{F}(\phi) = 0$ if $W + \tilde{A}^2 \cos^2 \phi/4 = W_0 \approx 1.43$. The function $\mathcal{F}(\phi)$ close to this point can be expanded in a Taylor series as $\mathcal{F}(\phi) \approx C_\beta(\beta_1 - \beta_{1,0}) = C_\beta(\sqrt{W + \tilde{A}^2 \cos^2 \phi/4} - \sqrt{W_0})$ [one can directly verify that $\mathcal{F}(\phi)$ is approximately linear in $\beta_1 = \sqrt{W + \tilde{A}^2 \cos^2 \phi/4}$, but not in W]. Using this expression in Eq. (13), one finds that the minimum of the functional Φ is achieved at $W = W_0 - \tilde{A}^2/4$ with an accuracy of $O(\tilde{A}^4)$, that is, the solution we are

searching for. Returning to the initial variables, the generation frequency can be expressed as

$$\omega = \omega_0 + 1.43\omega_M \frac{\tilde{\lambda}^2}{R_{\text{eff}}^2} - \omega_M \frac{\tilde{D}^2}{4\tilde{\lambda}^2}. \quad (16)$$

The threshold current density is found after the addition of the Gilbert damping contribution. In the range of small values of the Gilbert damping (compared to the radiation losses) this contribution is simply equal to $\sigma J_G = \alpha_G \omega$ [16], because small damping does not change the spin-wave profiles, and, consequently, radiation losses. In this case its role is simply to increase the threshold current to the value $\sigma J = \sigma J_0 + \alpha_G \omega$, so that the “negative damping” in the active area $\Gamma_- = \sigma J - \alpha_G \omega$ reaches the threshold value $\Gamma_{-, \text{th}} = \sigma J_0$. Thus, summarizing all the contributions, the threshold current density turns out to be

$$\sigma J_{\text{th}} = 1.86\omega_M \frac{\tilde{\lambda}^2}{R_{\text{eff}}^2} + \alpha_G \omega. \quad (17)$$

Equations (16) and (17) are the central results of the presented analytical model. In the limit of a zero i -DMI, they are reduced to the ones derived in Ref. [16], as it should be.

E. Analysis of the obtained equations

According to Eq. (16), the presence of the i -DMI leads to a redshift of the generation frequency. This shift is *independent* of the geometry of the SHO active area, i.e., on R_{eff} , and is equal to $\Delta\omega = -\omega_M \tilde{D}^2 / 4\tilde{\lambda}^2$. The reason for the frequency shift is clear—the i -DMI results in a decrease of the minimum frequency in the spectrum of spin waves. Indeed, the expression for the spin-wave spectrum of Eq. (3) can be rewritten as

$$\omega_k = \omega_0 + \omega_M \tilde{\lambda}^2 [(k_x + \tilde{D}/2\tilde{\lambda}^2)^2 + k_y^2] - \omega_M \tilde{D}^2 / 4\tilde{\lambda}^2, \quad (18)$$

i.e., the spectrum is shifted in the k_x direction, and is lowered by a value of $\Delta\omega = -\omega_M \tilde{D}^2 / 4\tilde{\lambda}^2$. The last value is *exactly the same* as the redshift of the generation frequency. This is absolutely natural, because the exchange interaction results in a certain offset of the generation frequency from the minimum frequency in the spectrum. This offset is the same for any i -DMI, because the structure of the spectrum remains the same except for the k_x shift, to which the exchange interaction is not sensitive. Thus, one can expect that the redshift of the generation frequency $\Delta\omega = -\omega_M \tilde{D}^2 / 4\tilde{\lambda}^2$ remains the same in all the i -DMI range, not only in the range of relatively small values. Our simulations below confirm this expectation. Also, it becomes clear that in the one-dimensional case (nanowire along the x direction), the redshift is also given by the same expression, $\Delta\omega = -\omega_M \tilde{D}^2 / 4\tilde{\lambda}^2$, as shown by the exact one-dimensional analytical model in Ref. [41].

Above, we have also found that, in the absence of Gilbert damping, the generation threshold is independent of the i -DMI. In this case the threshold is determined by the compensation of the radiation losses Γ_{rad} . The radiation losses are proportional to the spin-wave group velocity given by Eq. (11), so the total radiation losses are obtained after integration over ϕ_k , and are proportional to $\Gamma_{\text{rad}} \sim \langle k \rangle$, where the averaged spin-wave wave number is given by Eq. (12). Substituting the expression

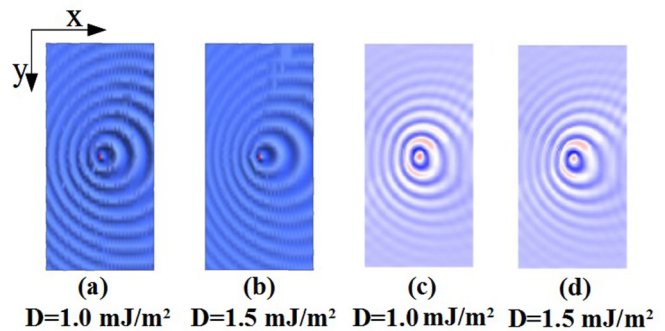


FIG. 2. Spatial profile of the excited spin-wave mode at different i -DMI strengths. (a) and (b) Theory [real part of the solution Eqs. (8) and (9)], and (c) and (d) micromagnetic simulations. The rectangular cross section is 1500 nm \times 3000 nm.

for the generation frequency [Eq. (16) into Eq. (12)], one finds that, in the range of relatively small i -DMI, $\langle k \rangle \approx k_0(1 - [\tilde{D}/(2k_0\tilde{\lambda}^2)]^4/4)$, where $k_0 = \sqrt{1.43}/R_{\text{eff}}$. In the above presented model we have neglected the terms of the order of \tilde{D}^4 . Thus, the radiation losses are independent of the i -DMI within the model, and, naturally, the obtained threshold current is also independent of the i -DMI. The expression for $\langle k \rangle$ gives also the range of the i -DMI, where the model is valid, $[\tilde{D}/(2k_0\tilde{\lambda}^2)]^4/4 \ll 1$. Outside this range, one may expect a decrease of the threshold current since the averaged group velocity decreases. Moreover, if $|\tilde{D}| > 2k_0\tilde{\lambda}^2$, spin waves in certain directions become nonpropagating (evanescent), since their wave vector becomes imaginary [see Eq. (10)]. This feature was observed in simulations in Ref. [42]. However, to calculate the threshold dependence on this region analytically, one should find a way to describe a general solution without an approximation of the small values of i -DMI, which lies beyond the scope of this paper.

IV. COMPARISON WITH MICROMAGNETIC SIMULATIONS AND DISCUSSION

In this section, we compare predictions of the above presented analytical model with the results of our micromagnetic simulations. The geometry and parameters of our micromagnetic simulations are described in Sec. II, and the value of the bias magnetic field was 400 mT. In this case the parameters determined by means of the analytical model are equal to a FMR frequency $\omega_0 = 2\pi \times 7.81$ GHz, effective exchange constant $\tilde{\lambda} = 5.64$ nm, and an effective i -DMI parameter $\tilde{D} = D \times 0.62$ nm, where D is expressed in mJ/m². The effective radius of the active region is estimated from the difference of the generation frequency from the FMR frequency in the absence of the i -DMI. In the simulations we found $\omega_0 = 2\pi \times 7.8$ GHz and $\omega_{\text{gen}} = 2\pi \times 8.7$ GHz, which, according to Eq. (16), results in the effective radius $R_{\text{eff}} = 42.2$ nm. The effective radius is close to the half distance between the concentrator tips, as should be expected.

First, in Fig. 2 we compare the analytical approximations Eqs. (8) and (9) of the profile of an excited spin-wave mode with the micromagnetic ones. One can clearly see that spin-wave profiles deviate from a purely cylindrical symmetry, and this

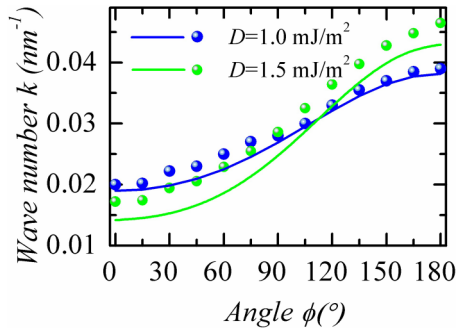


FIG. 3. Wave numbers of excited propagating spin-wave modes at different strengths of *i*-DMI. Symbols: micromagnetic simulation; lines: analytical expression [Eq. (10)].

deviation increases with the *i*-DMI, as expected. The analytical approximation describes micromagnetic spin-wave profiles reasonably well, and the weak deviation is related to the spatial distribution of the spin current, which is not of perfect radial symmetry (see, e.g., Supplemental Material in Ref. [41]), as was assumed in the model.

A quantitative comparison of the spin-wave profiles can be made via the calculation of the angular dependence of the spin-wave wave number (see Fig. 3). Analytically, this dependence is given by Eq. (10), in which one should calculate the generation frequency using Eq. (16). Micromagnetic dependence was found by a calculation of the distances between the zeros directly from the time evolution of the spatial distribution of the magnetization. The spin-wave wave number monotonically increases when the azimuthal angle is varied from $\phi = 0^\circ$ (+*x* direction) to $\phi = 180^\circ$ (−*x* direction); at negative angles the dependence is symmetric, $k(-\phi) = k(\phi)$. The maximum difference of the wave numbers $k(180^\circ) - k(0)$ is determined solely by the *i*-DMI strength, while the mean value mainly by the size of the active region. Again, we note quite a good description of the micromagnetic data by the analytical expression.

Next, we look at the dependence of the generation frequency on the *i*-DMI, which is shown in Fig. 4(a). Simulated frequencies follow the predicted trend, and decrease with the *i*-DMI as $\Delta\omega = -\omega_M \tilde{D}^2 / 4\tilde{\lambda}^2$. It should be noted that the equality of the characteristic contributions of the *i*-DMI and nonuniform exchange interaction, which corresponds to the condition $|\tilde{D}| = 2k_0\tilde{\lambda}^2$ [when the argument of the elliptic integral in Eq. (12) is equal to 1], in our case takes place at an *i*-DMI strength $D = 2.93$ mJ/m². Thus, the redshift of the generation frequency follows the same trend not only in the range of relatively small *i*-DMI values, but remains the same for a large *i*-DMI, as was predicted in Sec. III E.

Additionally, to prove this feature, we analyzed the data of micromagnetic simulation in Ref. [42], where STO with an active area of exactly circular shape was studied. We use the data presented for the smallest bias current (3 mA), for which the nonlinear effects should be small. In that case, the characteristic value of the *i*-DMI, when its effect becomes the same as the effect of an exchange interaction, is 0.85 mJ/m². As one can see from the inset in Fig. 4(a), the generation frequency follows the dependence of Eq. (16) in all the studied

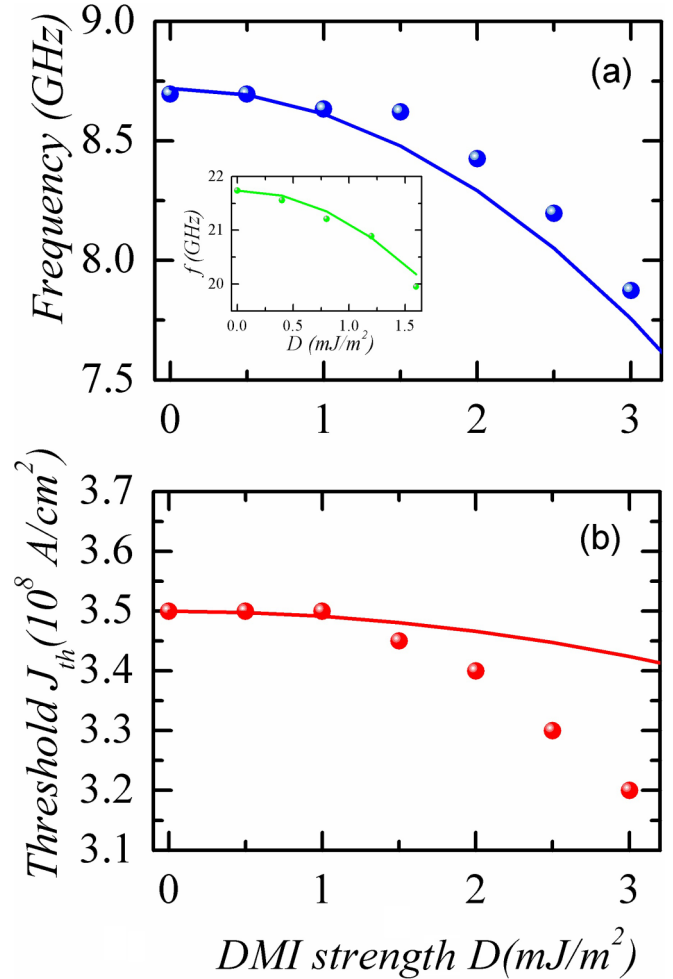


FIG. 4. Dependences of (a) the generation frequency and (b) threshold current density on the *i*-DMI strength. Symbols: micromagnetic data; lines: analytical model [Eqs. (16) and (17), respectively]. The inset in (a) shows the dependence of the generation frequency for the STO studied micromagnetically in Ref. [42]: Points are the micromagnetic data retrieved from Fig. 2(a) in Ref. [42] at a bias current of 3 mA, and the line shows the result of the analytical model [Eq. (16)].

i-DMI range, including the range where *i*-DMI becomes dominant ($D > 0.85$ mJ/m²).

For the calculation of the threshold current density [see Fig. 4(b)] one needs the value of the spin Hall efficiency $\sigma = \sigma_0 \sin\theta_M$. The theoretically calculated value is $\sigma_0 = 5.8 \times 10^{-3}$ m²/(A s). By determining the value of σ_0 from the matching of the calculated threshold by means of Eq. (17) in the absence of *i*-DMI and the micromagnetic data, we get a slightly higher value of $\sigma_0 = 6.6 \times 10^{-3}$ m²/(A s). This discrepancy is mainly attributed to a nonuniform spatial distribution of the current density, created by the concentrators. Below, we use the last value of the spin Hall efficiency for analytical calculations of the threshold current.

According to Eq. (17), which is valid in the range of relatively small *i*-DMI, the threshold current weakly depends on the *i*-DMI, because only the Gilbert losses are dependent on the *i*-DMI due to an *i*-DMI-induced redshift of the generation frequency, while the radiation losses do not depend

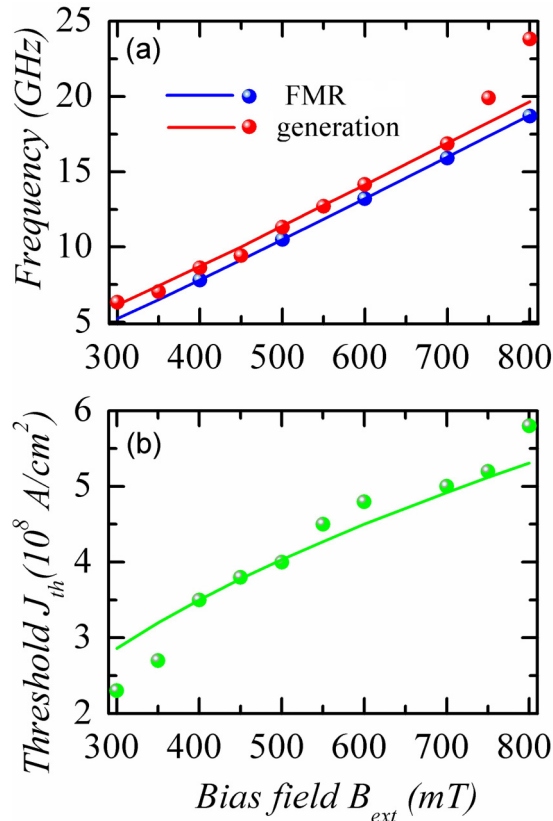


FIG. 5. (a) Frequency of FMR and frequency of the excited spin waves at the threshold as functions of the bias magnetic field. (b) Dependence of the threshold current on the bias magnetic field. Symbols: micromagnetic data; lines: analytical theory. The figures are plotted for the case of zero i -DMI.

on the i -DMI. In the range of relatively small i -DMI values ($D \leq 1.5$ mJ/m²) our micromagnetic simulations confirm this prediction. However, when the strength of the i -DMI becomes comparable to the strength of the exchange interaction, we observed a decrease of the generation threshold current. As was pointed out in Sec. III E, this decrease is related with a decrease of the averaged spin-wave group velocity, and, consequently, of the radiation losses.

Finally, we should note that the presented theory is rigorously valid for the STOs with a circular active region, while in the case of an SHO with concentrators one needs to use adjusting parameters, the effective radius R_{eff} and modified spin Hall efficiency σ . To check if these parameters are set solely by the geometry of the concentrators, we made simulations for different values of the bias magnetic field, which leads to a different magnetization angle, and compared these results with the corresponding curves calculated analytically. The i -DMI in this part of the study is not taken into account, since the effects of the i -DMI on the generation frequency and threshold do not depend on the R_{eff} [see Eqs. (16) and (17)]. As one can see from Fig. 5(a), the generation frequency has a constant offset from the FMR frequency, and it is almost perfectly described by the analytical expression Eq. (16) with a constant $R_{eff} = 42.2$ nm. The dependence of the threshold current density on the bias field [see Fig. 5(b)] also agrees very

well with the numerically calculated one in all the bias field range, especially noting that the accuracy of the determination of the critical parameters in simulations is often not very high, because of the properties of numerical noise. Summarizing this part, we found that the adjustable parameters of the analytical model are determined by the current density distribution, and could be found from one to two reference points of micromagnetic simulations.

V. CONCLUSIONS

In summary, in this paper, we have proposed an analytical model for the description of the excitation of two-dimensional nonreciprocal spin waves in spin torque and spin Hall oscillators in the presence of i -DMI. In the range of weak and moderate i -DMI the analytical problem of the spin-wave excitation is reduced to the eigenvalue problem for the generalized confluent Riemann equation. The profiles of the excited spin waves are described by a linear combination of a Laguerre's polynomial and a confluent hypergeometric function, and exhibit nonreciprocal behavior with the angular dependence of the spin-wave wave number.

It is shown that the frequency of the excited spin waves at the threshold exhibits a quadratic redshift with an increase of the i -DMI strength. This shift is a direct consequence of the lowering of the spin-wave spectrum bottom in the presence of the i -DMI. Therefore, this shift is proportional to the ratio between the characteristic i -DMI length and the exchange length, and could be expressed by the same functional dependence in all the studied i -DMI range, including the range where i -DMI makes a dominant contribution to the properties of the excited spin waves.

At the same time, the averaged spin-wave wave number and spin-wave group velocity are almost independent of the i -DMI in the range of small and moderate i -DMI. Consequently, the radiation losses remain the same, and the i -DMI affects the excitation threshold current only via its weak influence on the Gilbert losses, which are proportional to the generation frequency. However, when the effect of the i -DMI becomes comparable to or greater than that of the exchange interaction, we observed a decrease of the generation threshold, which is attributed to the decrease of the averaged group velocity.

ACKNOWLEDGMENTS

This work was supported by the executive programme of scientific and technological cooperation between Italy and China for the years 2016–2018 (code CN16GR09) title “Nanoscale broadband spin-transfer-torque microwave detector” funded by Ministero degli Affari Esteri e della Cooperazione Internazionale. This work was also supported in part by Grants No. EFMA-1641989 and No. ECCS-1708982 from the U.S. NSF, and by a DARPA M3IC grant under Contract No. W911-17-C-0031. R.Z. acknowledges support from the National Group of Mathematical Physics (GNFM-INdAM). R.V. acknowledges support from the Ministry of Education and Science of Ukraine (Project No. 0118U004007).

- [1] G. Bertotti, I. Mayergoyz, and C. Serpico, *Nonlinear Magnetization Dynamics in Nanosystems* (Elsevier, Amsterdam, 2009).
- [2] P. K. Muduli, O. G. Heinonen, and J. Åkerman, Decoherence and Mode Hopping in a Magnetic Tunnel Junction Based Spin Torque Oscillator, *Phys. Rev. Lett.* **108**, 207203 (2012).
- [3] G. Consolo, G. Finocchio, G. Siracusano, S. Bonetti, A. Eklund, J. Åkerman, and B. Azzèrboni, Non-stationary excitation of two localized spin-wave modes in a nano-contact spin torque oscillator, *J. Appl. Phys.* **114**, 153906 (2013).
- [4] A. Slavin and V. Tiberkevich, Nonlinear auto-oscillator theory of microwave generation by spin-polarized current, *IEEE Trans. Magn.* **45**, 1875 (2009).
- [5] Z. Zeng, G. Finocchio, and H. Jiang, Spin transfer nano-oscillators, *Nanoscale* **5**, 2219 (2013).
- [6] B. Wang, H. Kubota, K. Yakushiji, S. Tamaru, H. Arai, H. Imamura, A. Fukushima, and S. Yuasa, Diameter dependence of emission power in MgO-based nano-pillar spin-torque oscillators, *Appl. Phys. Lett.* **108**, 253502 (2016).
- [7] S. Tsunegi, K. Yakushiji, A. Fukushima, S. Yuasa, and H. Kubota, Microwave emission power exceeding 10 μ W in spin torque vortex oscillator, *Appl. Phys. Lett.* **109**, 252402 (2016).
- [8] L. Yang, R. Verba, V. Tiberkevich, T. Schneider, A. Smith, Z. Duan, B. Youngblood, K. Lenz, J. Lindner, A. N. Slavin, and I. N. Krivorotov, Reduction of phase noise in nanowire spin orbit torque oscillators, *Sci. Rep.* **5**, 16942 (2015).
- [9] A. Giordano, M. Carpentieri, A. Laudani, G. Gubbiotti, B. Azzèrboni, and G. Finocchio, Spin-Hall Nano-oscillator: A micromagnetic study, *Appl. Phys. Lett.* **105**, 042412 (2014).
- [10] V. Puliafito, A. Giordano, F. Garesci, M. Carpentieri, B. Azzèrboni, and G. Finocchio, Scalable synchronization of spin-Hall oscillators in out-of-plane field, *Appl. Phys. Lett.* **109**, 202402 (2016).
- [11] J. Torrejon, M. Riou, F. A. Araujo, S. Tsunegi, G. Khalsa, D. Querlioz, P. Bortolotti, V. Cros, K. Yakushiji, A. Fukushima, H. Kubota, S. Yuasa, M. D. Stiles, and J. Grollier, Neuromorphic computing with nanoscale spintronic oscillators, *Nature (London)* **547**, 428 (2017).
- [12] J. G. Zhu, X. Zhu, and Y. Tang, Microwave assisted magnetic recorder, *IEEE Trans. Magn.* **44**, 125 (2008).
- [13] M. V. Tsoi, A. G. M. Jansen, J. Bass, W. C. Chiang, M. Seck, V. Tsoi, and P. Wyder, Excitation of a Magnetic Multilayer by an Electric Current, *Phys. Rev. Lett.* **80**, 4281 (1998); Erratum: Excitation of a Magnetic Multilayer by an Electric Current, **81**, 493(E) (1998).
- [14] V. E. Demidov *et al.*, Magnetic nano-oscillator driven by pure spin current, *Nat. Mater.* **11**, 1028 (2012).
- [15] V. E. Demidov, S. Urazhdin, A. Zhodud, A. V. Sadovnikov, A. N. Slavin, and S. O. Demokritov, Spin-current nano-oscillator based on nonlocal spin injection, *Sci. Rep.* **5**, 8578 (2015).
- [16] J. C. Slonczewski, Excitation of spin waves by an electric current, *J. Magn. Magn. Mater.* **195**, L261 (1999).
- [17] L. Berger, Emission of spin waves by a magnetic multilayer traversed by a current, *Phys. Rev. B* **54**, 9353 (1996).
- [18] M. A. Hofer, M. J. Ablowitz, B. Ilan, M. R. Pufall, and T. J. Silva, Theory of Magnetodynamics Induced by Spin Torque in Perpendicularly Magnetized Thin Films, *Phys. Rev. Lett.* **95**, 267206 (2005).
- [19] S. Bonetti, V. Tiberkevich, G. Consolo, G. Finocchio, P. Muduli, F. Mancoff, A. Slavin, and J. Åkerman, Experimental Evidence of Self-Localized and Propagating Spin Wave Modes in Obliquely Magnetized Current-Driven Nanocontacts, *Phys. Rev. Lett.* **105**, 217204 (2010).
- [20] V. E. Demidov, S. Urazhdin, and S. O. Demokritov, Direct observation and mapping of spin waves emitted by spin-torque nano-oscillators, *Nat. Mater.* **9**, 984 (2010).
- [21] T. J. Silva and W. H. Rippard, Developments in nano-oscillators based upon spin-transfer point-contact devices, *J. Magn. Magn. Mater.* **320**, 1260 (2008).
- [22] Z. Duan *et al.*, Nanowire spin torque oscillator driven by spin orbit torques, *Nat. Commun.* **5**, 5616 (2014).
- [23] G. Consolo, L. Lopez-Diaz, B. Azzèrboni, I. Krivorotov, V. Tiberkevich, and A. Slavin, Excitation of Spin Waves by a Current-Driven Magnetic Nanocontact in a Perpendicularly Magnetized Waveguide, *Phys. Rev. B* **88**, 014417 (2013).
- [24] V. E. Demidov, S. Urazhdin, R. Liu, B. Divinskiy, A. Telegin, and S. O. Demokritov, Excitation of coherent propagating spin waves by pure spin currents, *Nat. Commun.* **7**, 10446 (2016).
- [25] T. Schneider, A. A. Serga, B. Leven, B. Hillebrands, R. L. Stamps, and M. P. Kostylev, Realization of spin-wave logic gates, *Appl. Phys. Lett.* **92**, 022505 (2008).
- [26] B. Lenk, H. Ulrichs, F. Garbs, and M. Münzenberg, The building blocks of magnonics, *Phys. Rep.* **507**, 107 (2011).
- [27] A. N. Slavin and V. S. Tiberkevich, Theory of mutual phase locking of spin-torque nanosized oscillators, *Phys. Rev. B* **74**, 104401 (2006).
- [28] S. Kaka, M. R. Pufall, W. H. Rippard, T. J. Silva, S. E. Russek, and J. A. Katine, Mutual phase-locking of microwave spin torque nano-oscillators, *Nature (London)* **437**, 389 (2005).
- [29] A. Houshang, E. Iacocca, P. Dürrenfeld, S. R. Sani, J. Åkerman, and R. K. Dumas, Spin-wave-beam driven synchronization of nanocontact spin-torque oscillators, *Nat. Nanotechnol.* **11**, 280 (2016).
- [30] I. Dzyaloshinskii, A thermodynamic theory of “weak” ferromagnetism of antiferromagnetics, *J. Phys. Chem. Solids* **4**, 241 (1958).
- [31] T. Moriya, New Mechanism of Anisotropic Superexchange Interaction, *Phys. Rev. Lett.* **4**, 228 (1960).
- [32] L. Udvardi and L. Szunyogh, Chiral Asymmetry of the Spin-Wave Spectra in Ultrathin Magnetic Films, *Phys. Rev. Lett.* **102**, 207204 (2009).
- [33] J.-H. Moon, S.-M. Seo, K.-J. Lee, K.-W. Kim, J. Ryu, H.-W. Lee, R. D. McMichael, and M. D. Stiles, Spin-wave propagation in the presence of interfacial Dzyaloshinskii-Moriya interaction, *Phys. Rev. B* **88**, 184404 (2013).
- [34] A. A. Stashkevich, M. Belmeguenai, Y. Roussigné, S. M. Cherif, M. Kostylev, M. Gabor, D. Lacour, C. Tiusan, and M. Hehn, Experimental study of spin-wave dispersion in Py/Pt film structures in the presence of an interface Dzyaloshinskii-Moriya interaction, *Phys. Rev. B* **91**, 214409 (2015).
- [35] K. Di, V. Li Zhang, H. Siah Lim, S. Choon Ng, M. Hau Kuok, X. Qiu, and H. Yang, Asymmetric spin-wave dispersion due to Dzyaloshinskii-Moriya interaction in an ultrathin Pt/CoFeB film, *Appl. Phys. Lett.* **106**, 052403 (2015).
- [36] S. Tacchi, R. E. Troncoso, M. Ahlberg, G. Gubbiotti, M. Madami, J. Åkerman, and P. Landeros, Interfacial Dzyaloshinskii-Moriya Interaction in Pt/CoFeB films: Effect of the Heavy-Metal Thickness, *Phys. Rev. Lett.* **118**, 147201 (2017).

- [37] R. Verba, V. Tiberkevich, and A. Slavin, Influence of interfacial Dzyaloshinskii-Moriya interaction on the parametric amplification of spin waves, *Appl. Phys. Lett.* **107**, 112402 (2015).
- [38] F. Garcia-Sanchez, P. Borys, A. Vansteenkiste, J.-V. Kim, and R. L. Stamps, Nonreciprocal spin-wave channeling along textures driven by the Dzyaloshinskii-Moriya interaction, *Phys. Rev. B* **89**, 224408 (2014).
- [39] J. H. Kwon, J. Yoon, P. Deorani, J. M. Lee, J. Sinha, K.-J. Lee, M. Hayashi, and H. Yang, Giant nonreciprocal emission of spin waves in Ta/Py bilayers, *Sci. Adv.* **2**, e1501892 (2016).
- [40] T. Brächer, O. Boulle, G. Gaudin, and P. Pirro, Creation of unidirectional spin-wave emitters by utilizing interfacial Dzyaloshinskii-Moriya interaction, *Phys. Rev. B* **95**, 064429 (2017).
- [41] A. Giordano *et al.*, Spin-Hall nano-oscillator with oblique magnetization and Dzyaloshinskii-Moriya interaction as generator of skyrmions and nonreciprocal spin-waves, *Sci. Rep.* **6**, 36020 (2016).
- [42] L. Yang, P. Dürrenfeld, X. Ruan, W. Liu, L. He, Y. Xu, and Y. Zhou, Directional Spin Wave in Spin-Torque Oscillators Induced by Interfacial Dzyaloshinskii-Moriya Interaction, *IEEE Magn. Lett.* **8**, 3509504 (2017).
- [43] R. K. Dumas, E. Iacocca, S. Bonetti, S. R. Sani, S. M. Mohseni, A. Eklund, J. Persson, O. Heinonen, and J. Åkerman, Spin-Wave-Mode Coexistence on the Nanoscale: A Consequence of the Oersted-Field-Induced Asymmetric Energy Landscape, *Phys. Rev. Lett.* **110**, 257202 (2013).
- [44] M. Cubukcu, J. Sampaio, K. Bouzehouane, D. Apalkov, A. V. Khvalkovskiy, V. Cros, and N. Reyren, Dzyaloshinskii-Moriya anisotropy in nanomagnets with in-plane magnetization, *Phys. Rev. B* **93**, 020401(R) (2016).
- [45] L. Lopez-Diaz, D. Aurelio, L. Torres, E. Martinez, M. A. Hernandez-Lopez, J. Gomez, O. Alejos, M. Carpentieri, G. Finocchio, and G. Consolo, *J. Phys. D: Appl. Phys.* **45**, 323001 (2012).
- [46] D. Cortés-Ortuño and P. Landeros, Influence of the Dzyaloshinskii-Moriya interaction on the spin-wave spectra of thin films, *J. Phys.: Condens. Matter* **25**, 156001 (2013).
- [47] V. V. Naletov, G. de Loubens, G. Albuquerque, S. Borlenghi, V. Cros, G. Faini, J. Grollier, H. Hurdequint, N. Locatelli, B. Pigeau, A. N. Slavin, V. S. Tiberkevich, C. Ulysse, T. Valet, and O. Klein, Identification and selection rules of the spin-wave eigenmodes in a normally magnetized nanopillar, *Phys. Rev. B* **84**, 224423 (2011).
- [48] We use the definition of complex magnetization variable a , conjugated comparing to Ref. [16]. This results in the change of sign before the damping term in Eq. (4) and a consequent change of the Hankel function in our work to the one in Ref. [16].
- [49] E. A. Vlasova, V. S. Zarubin, and G. N. Kuvyrkin, *Approximate Methods of Mathematical Physics* (MSTU publishing, Moscow, 2001).
- [50] T. Zhu and S. N. Atluri, A modified collocation method and a penalty formulation for enforcing the essential boundary conditions in the element free Galerkin method, *Comput. Mech.* **21**, 211 (1998).
- [51] J. C. Newman, An improved method of collocation for the stress analysis of cracked plates with various shaped boundaries, NASA Technical Note D-6376, 1971.